JBC Papers in Press. Published on October 19, 2009 as Manuscript M109.048330
The latest version is at http://www.jbc.org/cgi/doi/10.1074/jbc.M109.048330

IDENTIFICATION OF SMARCAL1 AS A COMPONENT OF THE DNA DAMAGE RESPONSE

Lisa Postow[1], Eileen M. Woo[1,2], Brian T. Chait[2], and Hironori Funabiki[1]
From Laboratory of Chromosome and Cell Biology[1], and Laboratory of Mass Spectrometry and Gaseous Ion Chemistry[2],
The Rockefeller University, New York, NY 10065
Running head: SMARCAL1 is a DNA damage protein
Address correspondence to: Lisa Postow, 1230 York Avenue, New York, NY 10065. Fax: 212-327-7292; E-mail: PostowL@rockefeller.edu

SMARCAL1 (also known as HARP) is a SWI/SNF family protein with an ATPase activity stimulated by DNA containing both single-stranded and double-stranded regions. Mutations in SMARCAL1 are associated with the disease Schimke immuno-osseous dysplasia (SIOD), a multisystem autosomal recessive disorder characterized by T cell immunodeficiency, growth inhibition, and renal dysfunction. The cellular function of SMARCAL1, however, is unknown. Here, using *Xenopus* egg extracts and mass spectrometry, we identify SMARCAL1 as a protein recruited to double-strand DNA breaks. SMARCAL1 binds to double-strand breaks and stalled replication forks in both egg extract and human cells, specifically colocalizing with the single-stranded DNA binding factor RPA. In addition, SMARCAL1 interacts physically with RPA independently of DNA. SMARCAL1 is phosphorylated in a caffeine-sensitive manner in response to double-strand breaks and stalled replication forks. It has been suggested that stalled forks can be stabilized by a mechanism involving caffeine-sensitive kinases, or they collapse and subsequently recruit Rad51 to promote homologous recombination repair. We show that depletion of SMARCAL1 from U2OS cells leads to increased frequency of RAD51 foci upon generation of stalled replication forks, indicating that fork break-down is more prevalent in the absence of SMARCAL1. We propose that SMARCAL1 is a novel DNA damage-binding protein involved in replication fork stabilization.

The cellular response to DNA damage is a complicated meshwork of pathways that have evolved to halt the progression of the cell cycle and process and repair the damaged DNA (1). A critical component in a number of these DNA damage response pathways, including the response to double-strand breaks (DSBs) and stalled replication forks, is single-stranded DNA (ssDNA) coated with the ssDNA binding factor replication protein A (RPA), a heterotrimer consisting of 70, 32, and 14 kDa subunits (2). ssDNA accumulates following DSB formation due to resection by nucleases and helicases and is quickly coated in RPA filaments (3). RPA is replaced subsequently with RAD51, which initiates strand exchange in the homologous recombination pathway. In addition to its role in DNA repair, RPA-coated ssDNA is believed to provide a binding site for the ATM and Rad3-related kinase (ATR) and the ATR interacting protein (ATRIP), allowing the activation of ATR and initiation of damage checkpoint and repair pathways (4).

Long tracts of ssDNA also form at stalled replication forks by the dissociation of replicative helicases from stalled DNA polymerases (5,6). RPA-coated ssDNA helps to activate the ATR-dependent replication checkpoint, which stabilizes stalled forks (7). In the absence of the replication checkpoint in yeast, stalled forks convert to aberrant structures detectable by two dimensional agarose gel electrophoresis (8). At least some of these structures, as observed by electron microscopy, are four-way junctions resulting from annealing the complementary daughter strands, called reversed forks or chickenfoot structures (9). A chickenfoot can be resolved by a Holliday junction endonuclease to create a DSB, which must then be repaired, following recruitment of RAD51, by homologous recombination. However, the exact mechanisms that control replication fork stabilization and the steps of fork collapse remain unclear.

To better understand the proteins and dynamics involved in the DNA damage response, we used extract from the eggs of the frog *Xenopus laevis* to identify proteins bound to DSBs (10). By incubating linearized plasmid bound to

streptavidin-coated magnetic beads in egg extract, we were able to isolate DNA damage response complexes. These complexes could then be analyzed using mass spectrometry (MS) and other biochemical tools. Using this approach, we have identified SWI/SNF related, matrix associated, actin dependent regulator of chromatin, subfamily a-like 1 (SMARCAL1) as a novel DSB binding protein.

SMARCAL1, also known as HepA related protein (HARP) and DNA-dependent ATPase A, was originally identified as an ATPase activity biochemically isolated from calf thymus (11). The SMARCAL1 ATPase is stimulated by DNA containing both ssDNA and double-stranded DNA (dsDNA) regions (12,13). SMARCAL1 exists in species ranging from *Caenorhabditis elegans* to humans, but there is no yeast homologue. It contains a C-terminal SWI/SNF helicase domain as well as HARP homology domains. The SMARCAL1 SWI/SNF subfamily is most closely related to the prokaryotic HepA/RapA SWI/SNF subfamily (12). HepA/RapA is an RNA polymerase-associated protein suggested to be involved in recycling transcription complexes (14).

Recently, it has been shown that purified SMARCAL1 is able to catalyze the re-annealing of single-stranded regions of a plasmid that are held apart by RPA (15). This led to the proposal that SMARCAL1 is an "annealing helicase," as it has not been observed to have strand separation activity. SMARCAL1 has also been identified as the gene responsible for the autosomal-recessive multisystem disorder Schimke immuno-osseous dysplasia (SIOD) (16). SIOD is characterized by T-cell immunodeficiency, renal dysfunction, and growth failure, among other phenotypes (17). The cellular function of SMARCAL1, however, remains unknown.

We show here that SMARCAL1 is a component of the DNA damage response. We demonstrate that it interacts with damaged DNA and stalled replication forks in both *Xenopus* egg extract and human nuclei, and that it specifically colocalizes with and interacts with RPA. SMARCAL1 contains at its N-terminus a motif known to interact with the C-terminal domain of RPA32, and this sequence is required for SMARCAL1 to bind to DSBs. In addition, SMARCAL1 becomes phosphorylated in response to the DNA damage checkpoint response. Finally, collapse of stalled replication forks appears to be more frequent in the absence of SMARCAL1. We propose that SMARCAL1 is a novel DNA damage-binding protein, and that it plays a role in the stabilization of stalled replication forks. A possible role for this function in the phenotype of SIOD is discussed.

EXPERIMENTAL PROCEDURES

Xenopus laevis egg extract- Meiotic metaphase II-arrested (CSF) *Xenopus laevis* egg extract was prepared as described (18). Where indicated, 300 μM aphidicolin (Sigma), 220 nM destruction box-deleted geminin (19) (generated from a plasmid provided by W.M. Michael), or 5 mM caffeine (Sigma) were added to the extract. For spin-down experiments, sperm nuclei (4000 /μl) were incubated in interphase extract for one hour, and chromatin was purified by spinning through a 30% sucrose cushion as described (20). Geminin was added before, and aphidicolin 15 minutes after, the addition of sperm nuclei to extract. DNA bead experiments have been described, as have the single biotin, double biotin, single hairpin, and double stranded DNA beads (10). For all DNA bead experiments, 1 μg DNA bound to beads was incubated with 50 μl extract for 30 minutes at 22 ^{o}C. The double hairpin DNA is a circular permutation of the single hairpin DNA, and was made by self-annealing the oligo 5'-/5Phos/GAG CTA AGC TGG T/iBiodT/A CAG CTT AGC TCC AGA TCC TCG TTA GAG GAT CTG-3'. The ssDNA oligo was 5'-GCT GAA CCG GTA CGC CTT TCT CCC TTC GGG AAG CGT GGC GCT TTC TCC/3Bio/-3'. All DNA oligos were purchased from IDT. For immunodepletions, anti-xSMARCAL1 antibodies were bound to protein A-coated magnetic beads (Invitrogen) according to instructions and incubated in egg extract on ice for two rounds of 45 minutes each.

In vitro translation- Clones containing xSMARCAL1 (IMAGE: 6323401) and xSNF2L (IMAGE: 6317687) were purchased from Open Biosystems. SMARCAL1-FLAG was cloned into pCS2+ using the oligos 5'-CGA ATT CAA GGC CTC TCG AGA TGT CCG TCT GTC TGA CGG A-3' and 5'-CGA CTC ACT ATA GTT CTA GAT TAT TTA TCA TCA TCA TCT TTA TAA

TCT CCT CCC AGT GCA AAG TAA TCG TCA A-3'. ΔN-xSMARCAL1-FLAG was cloned using the upstream primer 5'-CGA ATT CAA GGC CTC TCG AGA TGA GTC CAA AAA AGA AAC GAA AAG TAG GAG GAT CCA CTC TGT TTA ACA TCC AG-3', which replaces the first 42 amino acids with the nuclear localization signal of the SV40 large T antigen. The 4AQ mutant was generated by sequential site-directed mutagenesis, using the oligos 5'-GTT AAA TCC TGC TTG CAC TGC CCA AGA ACA AGA AAG CCC AAG AA-3', 5'-CCA GAC CAG CCG AGC TGT ACG CAC AGA TTG CTG CCG TCA GA-3', 5'-GTC ATT GTG ACT GGA CGA GAC GCC CAG AGC GCC AAT CTG ATC AA-3', and 5'-GAT TGA AAT CCG AGG TCC TGG CCC AGC TTC CCG CTA AAC AG-3', and their complements. In vitro translation was in rabbit reticulocyte lysate using the SP6 and T7 RNA polymerases according to the manufacturer's instructions (Promega).

Cell culture- U2OS cells were purchased from ATCC and were grown according to instructions. Where indicated, 5 mM caffeine or 4 mM hydroxyurea (Sigma) was added to the media. siRNAs were purchased from Thermo Scientific. As a control, we used the ON-TARGETplus Non-targeting Pool, which contains four separate siRNAs designed to not target any gene (Dharmacon), and to deplete hSMARCAL1 we used siRNAs (Dharmacon) targeting the sequences 5'-GCU UUG ACC UUC UUA GCA A-3' (siRNA#1) and 5'-AAG CAA GGC CCA UCC CAA A-3' (siRNA#2). siRNAs were transfected into U2OS cells using the Lipofectamine RNAiMAX reagent (Invitrogen). Cells were transfected twice, two days apart, and were split for experiments the day following the second transfection. The next day, when cells were 30-50% confluent, hydroxyurea was added and cells were collected for lysis or fixed for microscopy after 24 hours. For microcopy, cells were plated onto poly-lysine-coated coverslips, fixed in 2% paraformaldehyde, and permeabilized with 0.5% NP-40.

To make cells expressing hSMARCAL1-GFP, hSMARCAL1 (from IMAGE: 6058575) was cloned into pEA24, a retroviral C-terminal eGFP vector that was the generous gift of Emily Foley and Tarun Kapoor. The gene was integrated into the genome of U2OS cells using retroviral transduction.

Antibodies- Antibodies against hRPA32 (ab16855), H3 (ab1791) and hSMARCAL1 (ab69900) were purchased from Abcam; anti-hRAD51 (sc-8349) and anti-PCNA (sc0-56) from Santa Cruz Biotechnology; antibodies against phosphorylated S345 of hCHK1 (2341) from Cell Signaling; against γH2AX (05-636) from Millipore; against FLAG (M2) and tubulin (DM1) from Sigma. Mouse anti-GFP (11814460001) was purchased from Roche and rabbit anti-GFP was a gift from Tarun Kapoor and Emily Foley. Rabbit anti-xRPA70 was a gift from Yasuhisa Adachi. Rabbit anti-xSMARCAL was produced against the peptide CKDFTSSKNLTGKYVAPKA, and rabbit anti-xCIRP2 was produced against GST-xCIRP2 purified out of *Escherichia coli*. Anti-SKP1 and anti-xKu70 were previously described (10).

For immunoprecipitations, antibodies were attached to magnetic beads coated in protein A or protein G (Invitrogen). For anti-FLAG immunoprecipitations, 85 μl extract was mixed with 15 μl rabbit reticulocyte lysate containing translated xSMARCAL1-FLAG or a mock reticulocyte lysate control reaction. Antibody beads were incubated with extract for one hour on ice and washed with phosphate buffered saline with 0.1% triton X-100.

Mass spectrometry- Tandem MS (MS/MS) was as described (10). Proteins were identified using the Xproteo search engine (www.xproteo.com).

RESULTS

Identification of xSMARCAL1 as a novel damage binding protein in Xenopus laevis *egg extract.* Previously, we developed a method to isolate damage-binding complexes from *Xenopus laevis* egg extract (10). In this approach, we employed biotinylated DNA with various features bound to magnetic streptavidin-coated beads. Linearized plasmid DNA biotinylated on one end (single biotin DNA, or SB-DNA) modeled a DSB when bound to beads, whereas when both DNA ends were biotinylated (double biotin DNA, or DB-DNA), the ends were obscured by the bead (Fig. 1A). We previously observed that SB-DNA beads interacted specifically with numerous damage-binding proteins including xKu70, xKu80, xMre11, and xRPA70; initiated the

phosphorylation of the frog CHK2 homologue xCDS1 in response to checkpoint activation; and were good substrates for the nonhomologous end joining repair pathway. In contrast, DB-DNA beads bound many chromatin-associated proteins but did not model a DSB in extract.

MS/MS analysis revealed three peptides of the protein xSMARCAL1, a SWI/SNF family ATPase associated with the disease SIOD, specifically in the SB-DNA bead sample (Supplemental Table S1). To confirm the MS/MS results, we expressed xSMARCAL1 in rabbit reticulocyte lysate in the presence of ^{35}S-methionine, mixed this with egg extract, incubated it with beads, and analyzed radioactive protein co-isolating with beads by gel electrophoresis. We found that xSMARCAL1 was able to interact strongly with SB- but only weakly with DB-DNA beads, a bias that was not observed for the control protein histone H3 (Fig. 1B). In contrast, the chromatin remodeling protein xSNF2L interacted strongly with both SB- and DB-DNA beads (Fig. 1C).

Purified SMARCAL1 has been shown in vitro to interact with DNAs that contain both ssDNA and dsDNA regions (11-13,15). To understand SMARCAL1 binding preferences in a more physiological context, we analyzed its interactions with a series of DNA substrates (see Fig. 1A). These substrates had been designed to model DNAs with different structural features. As stated above DB-DNA models undamaged chromatin, while SB-DNA models a chromosomal DSB. We also used oligo DNA beads, which have different binding preferences for marker proteins that give indications of DNA structure. We used three marker proteins: xKu70, which will only strongly bind dsDNA with an accessible end; the histone H3, which binds to dsDNA long enough to form a nucleosome; and the RNA-binding protein xCIRP2 (21), which interacts with ssDNA in egg extract (L.P. and H.F., unpublished data). We found that, in addition to SB-DNA beads, xSMARCAL1 binds strongly to single hairpin DNA (SH-DNA), which contain 55% G and C and can become frayed in the extract, as evidenced by its ability to bind xCIRP2. xSMARCAL1 binds much more weakly to a nearly identical DNA that contains a second hairpin (double hairpin DNA, or DH-DNA) and therefore cannot breathe or bind strongly to xCIRP2 (Fig. 2A). In addition, xSMARCAL1 binds weakly to a 49 bp double-stranded oligo (double strand DNA, or DS-DNA) that is capped by 4 G-C base pairs and has an overall G-C content of 63%. Finally, xSMARCAL1 has almost no binding to a 48-mer single-stranded oligo (single strand DNA, or SS-DNA). In short, our results in extract indicate that, in a physiological context, xSMARCAL1 has a strong preference for DNA ends that have the ability to contain both ssDNA and dsDNA regions.

hSMARCAL1 colocalizes with hRPA at DSBs in mammalian nuclei. Binding of xSMARCAL1 to SB-DNA beads suggested that its human homologue, with which it shares 55% amino acid identity, would bind to DSBs in the nuclei of human cells. To monitor hSMARCAL1 localization, we used a U2OS cell line stably expressing hSMARCAL1 fused at its C-terminus to GFP. Anti-GFP antibodies detected some hSMARCAL1-GFP foci in undamaged cells. Damage-dependent foci began to form within an hour after treating the cells with 10 Gy of gamma irradiation and increased in intensity in the hours following treatment (Fig. 2A).

hSMARCAL1-GFP foci colocalized with a subset of γH2AX foci, indicating that the foci do indeed represent DSBs (Fig. 2B and C). Because xSMARCAL1 interacted with DNA containing ssDNA regions in egg extract, we next compared hSMARCAL1 localization to that of the two major single-stranded binding factors in the damage response: hRPA and hRAD51. To detect hRPA foci, we used an antibody against the 32 kDa subunit, hRPA32. While hSMARCAL1-GFP foci colocalized with a subset of hRAD51 foci, their localization corresponded nearly precisely with that of hRPA32 (Fig. 2B and C). Colocalization of endogenous hSMARCAL1 and hRPA was also seen using a polyclonal antibody against hSMARCAL1 (Supplemental Fig. S1).

xSMARCAL1 and hSMARCAL1accumulate at stalled replication forks. Based on the DNA structural preferences of SMARCAL1, we speculated that it might bind to replication forks. To test this directly, we isolated sperm chromatin that had been incubated in interphase *Xenopus* egg extract to induce replication. Stalled replication forks were generated by inhibiting DNA polymerases with aphidicolin, while unreplicated chromosomes were prepared by adding recombinant replication initiation inhibitor

geminin (19). Chromosomes were enriched from these extracts, and associated xSMARCAL1 was detected using anti-xSMARCAL1 antibodies. As controls, we used antibodies recognizing xH3, which binds to all chromatin irrespective of replication initiation; xPCNA, the replication clamp protein, which becomes characteristically mono- or di-ubiquitylated, depending on the state of the replication fork; and xRPA70. As has been seen previously, xPCNA became mono-ubiquitylated upon DNA replication and di-ubiquitylated upon treatment with aphidicolin (22). Both xSMARCAL1 and xRPA70 had little affinity for chromatin in geminin-treated extract, as similar amounts of both proteins were sedimented in control extract lacking sperm chromatin. While xSMARCAL1 and xRPA70 had some affinity for replicating DNA, both proteins bound strongly to chromatin containing forks stalled with aphidicolin (Fig. 3A and B). We conclude that xSMARCAL1 preferentially accumulates on stalled replication forks.

Next, we looked at the localization of hSMARCAL1 at stalled forks in U2OS cells. We first observed that hSMARCAL1-GFP colocalized with hRPA32 foci in undamaged cells (Fig. 3C), and we speculated that these foci represented stalled replication forks occurring during normal replication. To further confirm that hSMARCAL1 associates with stalled replication forks in mammalian cells, we treated U2OS cells with 4 mM hydroxyurea (HU), which depletes dNTPs from the cell by inhibiting the enzyme ribonucleotide reductase, thereby stalling forks. Again, we observed the colocalization of hRPA32 with hSMARCAL1-GFP (Fig. 3D). Indeed, in the vast majority of cells, greater than 60% of detectable hRPA32 foci colocalized with hSMARCAL1-GFP foci (Fig. 3E), demonstrating that SMARCAL1 preferentially binds to the same DNA substrates as RPA.

xSMARCAL1 interacts with xRPA. The colocalization of SMARCAL1 with RPA led us to hypothesize that the two proteins might interact physically. Many ssDNA-binding proteins involved in the DNA damage response also interact physically with RPA (2). These include RAD51 (23) and the Werner syndrome and Bloom syndrome helicases (WRN and BLM) (24-26). In addition, several of these proteins, including the base excision repair protein UNG2 and the nucleotide excision repair protein XPA, contain a motif that specifically interacts with the C-terminal domain of RPA32 (27). We noticed that the very N-terminus of SMARCAL1, which is extremely well conserved among species as opposed to the N-terminal region as a whole, contains a similar motif. This sequence is also highly similar to a sequence in TIPIN, a stalled replication fork-binding protein known to interact with RPA (28), and to one in Rad14, the yeast XPA homologue (Fig. 4A). This region of SMARCAL1 is thought to contain its nuclear localization signal (12).

To investigate a possible physical interaction between SMARCAL1 and RPA, endogenous xSMARCAL1 was immunoprecipitated out of egg extract in the absence of DNA, and xRPA70 protein indeed co-immunoprecipitated (Fig. 4B). It was possible that xRPA70 was binding to our anti-xSMARCAL1 antibody independently of xSMARCAL1. To eliminate this possibility, we added in vitro translated C-terminally FLAG-tagged xSMARCAL1 to extract and isolated complexes with anti-FLAG antibodies. Anti-FLAG antibodies co-isolated xRPA70 only when xSMARCAL1-FLAG was added to extract (Fig. 4C). As a control, we immunoblotted using an anti-SKP1 antibody. As expected, xSKP1 interacted in a similarly weak manner with anti-FLAG antibodies either in the presence or absence of xSMARCAL1-FLAG.

To test the importance of the N-terminal motif, we replaced the N-terminal 42 amino acids of xSMARCAL1-FLAG with the SV40 large T antigen nuclear localization signal. We then immunodepleted more than 97% of endogenous xSMARCAL1 out of extracts, and replaced it with in vitro translated xSMARCAL1-FLAG or ΔN-xSMARCAL1-FLAG (Fig. 4D). The truncated protein retained its ability to bind RPA (Fig. 4E), likely through an additional interaction with the RPA70 subunit (data not shown). Consistent with this observation, many proteins that interact with RPA are known to bind to more than one RPA subunit (2). We next tested the ability of the ΔN truncation to bind to DSBs. Surprisingly, ΔN-xSMARCAL1-FLAG retained almost no ability to bind to either SB-DNA or SH-DNA beads (Fig. 4F). In addition, ΔN-hSMARCAL1, also containing the large T antigen nuclear localization

signal, was unable to colocalize with hRPA foci in irradiated U2OS cells although it was efficiently imported into the nucleus (data not shown). While the exact role for this N-terminal sequence of SMARCAL1 remains unclear, it appears to be absolutely critical for the proper localization of the protein.

xSMARCAL1 and hSMARCAL1 are phosphorylated as a result of ATM and/or ATR activity. During the course of our investigation of xSMARCAL1 DNA-binding ability, we observed that xSMARCAL1 bound to SB-DNA beads in *Xenopus laevis* egg extract was shifted to a slightly lower mobility form relative to unbound protein (see Fig. 1B). This shift was not apparent on protein bound to SH-DNA beads, which are not long enough to induce xCDS1 phosphorylation (L.P. and H.F., unpublished data), nor did it occur on protein remaining in extract following isolation of DNA beads (Supplemental Fig. S2). These observations indicate that binding to structures recognized by the ATM or ATR pathways is required for this modification.

Checkpoint and many repair responses are regulated through the activation of the phosphoinositide-3-kinase family members ATM and ATR, both of which interact with damaged DNA and phosphorylate downstream effector proteins on serine and threonine residues. Caffeine is a potent inhibitor of ATM and ATR, and the altered mobility of xSMARCAL1 was abolished when extract contained caffeine (Fig. 5A).

Both ATM and ATR generally phosphorylate on the consensus sequence S/TQ (29-31), but they have also been shown to phosphorylate at alternative sequences (32). We mutated all four of the SQ and TQ sites in the xSMARCAL1 gene (T164, S359, T613, and S673) to create a 4AQ mutant. This mutant protein was expressed in reticulocyte lysate, added to egg extract, and incubated with SB-DNA beads in the presence or absence of caffeine. While caffeine abolished the shift, no difference in the modification pattern resulted in the 4AQ mutant (Fig. 5A), suggesting that xSMARCAL1 either is not directly phosphorylated by ATM or ATR, or that it is phosphorylated on a non-canonical site.

Since we had observed that SMARCAL1 interacted with stalled replication forks as well as DSBs, we investigated whether stalled forks also stimulated its modification. Following HU treatment of U2OS cells, hSMARCAL1 was shifted and this shift was lost upon λ phosphatase treatment (Fig. 5B). In a similar manner, antibodies specific for phosphorylated S345 of hCHK1 and hRPA32 detected phosphorylations following HU treatment that were removed after phosphatase treatment. Finally, we confirmed that hSMARCAL1 became phosphorylated in response to DSBs in human cells. U2OS cells were irradiated with 10 Gy. This caused a shift in the hSMARCAL1 band, which was inhibited by caffeine and abolished by λ phosphatase treatment (Fig. 5C).

Caffeine inhibits the ATM, ATR, and DNA-PK kinases, as well as others. To attempt to further demonstrate the role of damage checkpoints in SMARCAL1 phosphorylation, we used specific inhibitors of ATM and DNA-PK. DNA-PK inhibition did not inhibit hSMARCAL1 phosphorylation, while ATM inhibition did at early timepoints (data not shown). We believe that early ATM-dependent phosphorylation of hSMARCAL1 is likely at least partially due to the role ATM plays in stimulating end resection, RPA binding, and ATR activation (33). Taken together, the requirements for DNA binding, end resection, and DNA structures that activate the damage checkpoint, as well as the sensitivity of phosphorylation to caffeine, it seems likely that ATM and/or ATR is directly or indirectly responsible for the SMARCAL1 modification following its localization to DNA damage. Thus, this modification appears to be a component of the ATM- and ATR-dependent checkpoint and repair pathways.

hSMARCAL1 depletion leads to increased frequency of hRAD51 foci in HU-treated cells. The colocalization of SMARCAL1 and RPA and the phosphorylation of SMARCAL1 following HU treatment led us to hypothesize that the protein plays a role in fork stabilization. Replication forks are stabilized by the replication checkpoint, preventing the formation of alternative DNA structures including chickenfoot structures or DSBs that must be resolved through the homologous recombination pathway (34). In yeast, recombination proteins do not accumulate at stalled replication forks unless the replication checkpoint pathway has been lost (35,36), indicating that recombination proteins accumulate at forks only after they have broken down.

To test whether hSMARCAL1 is involved in replication fork stabilization, we used HU to stall replication forks in cells that had been treated with either nontargeting control siRNAs or with two siRNAs independently targeting the hSMARCAL1 gene. Each hSMARCAL1-specific siRNA depleted more than 94% of the endogenous protein (Fig. 6A). Anti-hRPA32 immunofluorescence following 24 hours of HU treatment revealed hundreds of bright foci in many nuclei, corresponding to the built-up ssDNA resulting from decoupling of helicases and polymerases at the stalled forks (7). In some cells, however, bright hRAD51 foci colocalized with hRPA32 foci (Fig. 6B). Bright hRAD51 foci likely represent forks that have broken down and either initiated the homologous recombination repair pathway or formed deleterious DNA structures.

In the absence of HU treatment, approximately 27% of nuclei contain more than 10 bright hRAD51 foci in both control and SMARCAL1-depleted cells (Fig. 6C). After HU treatment, the number of bright hRAD51-positive cells increased only very slightly in control cells. However, a significantly higher percentage of cells treated with both siRNA#1 and siRNA#2, 51% and 46% respectively, contained bright hRAD51 foci (Fig. 6D). These results suggest that hSMARCAL1-depleted cells have a higher proportion of broken-down replication forks in the presence of HU than control cells, and that hSMARCAL1 plays a role in replication fork stabilization.

DISCUSSION

The cell-free system of *Xenopus laevis* egg extract allows the purification and MS/MS analysis of DNA repair complexes, an important tool for the discovery of novel damage-binding proteins and post-translational modifications on damage-bound proteins. Here we described the use of this method to identify SMARCAL1 as a component of the DNA damage response. Our evidence for this is: first, SMARCAL1 binds to DSBs and stalled replication forks in vivo; second, it is phosphorylated as a result of the DNA damage checkpoint response following generation of DSBs and stalled forks; third, like many DNA damage response proteins, it interacts physically with the ssDNA binding factor RPA; and finally, the absence of SMARCAL1 enhances RAD51 association with stalled replication forks in mammalian cells, indicating that a greater number of broken forks are entering the homologous recombination pathway.

Recently, it has been shown that purified SMARCAL1 is capable of catalyzing the re-annealing of separated strands of a plasmid held apart by RPA molecules (15). The authors proposed that the enzyme acts directly on the DNA in the reverse reaction to that of a helicase, thus forcing off the RPA. Alternatively, SMARCAL1 may remove RPA from the DNA, allowing the complementary strands to anneal. Evidence against this model includes the observations that SMARCAL1 ATPase activity is not stimulated by RPA and that SMARCAL1 only removes RPA when the action is linked to annealing of complementary strands (15).

Our evidence suggests that SMARCAL1 is involved in replication fork stabilization, and the observed in vitro activity could play a role in this. An annealing helicase activity might help to stabilize stalled forks by maintaining daughter-parent strand pairing and preventing alternative DNA structures such as reversed forks (Fig. 7). Loss of this activity would lead to increased fork break-down, the generation of DSBs, and, consequently, RAD51 loading. Another possibility, however, is that SMARCAL1 acts after replication forks have collapsed. In this scenario, SMARCAL1 might be acting as an antagonist to RAD51 binding and homologous recombination. Further studies will be required to distinguish between these two possibilities.

Interestingly, we have found that SMARCAL1 contains an N-terminal motif known to interact with the 32 kDa subunit of RPA. While SMARCAL1 interacted with RPA in the absence of DNA, this motif was not required for this interaction. This observation is not necessarily surprising, as many proteins that interact with RPA do so with more than one subunit. More striking, however, was the fact that this N-terminal region was absolutely required for SMARCAL1 to bind to DSBs in both *Xenopus* egg extracts and U2OS cells. This observation is particularly surprising, because the N-terminal region of SMARCAL1 is not required for DNA-stimulated ATPase activity in vitro (13). It seems likely,

therefore, that an interaction with the RPA32 C-terminal domain is important for association of SMARCAL1 with damage in vivo, perhaps because RPA obscures ssDNA binding sites. RPA-coated DNA is not, however, sufficient for SMARCAL1-DNA interactions, as SMARCAL1 does not interact with SS-DNA beads, although RPA does (data not shown).

Many SWI/SNF family proteins are involved in the DNA damage response, including Rad54 (37), Ino80 (38), and the mammalian SWI/SNF complex (39). However, our observations of SMARCAL1 suggest that it is functionally more closely related to members of the RecQ helicase family. The RecQ helicases BLM and WRN show a localization pattern similar to that of SMARCAL1 and also physically interact with RPA (40). The sole RecQ family member in yeast, Sgs1, helps to prevent the formation of aberrant Rad51-dependent DNA structures at stalled replication forks (41). How RecQ helicases function to stabilize and/or repair stalled forks is still largely unknown (40). It has been suggested that BLM is involved in the formation or removal of chickenfoot structures (42), and both BLM and WRN can catalyze chickenfoot formation in vitro (42-44). In addition to helicase activity, RecQ proteins have intrinsic ATP-dependent strand annealing activity (45,46), which may be similar to the activity that Yusufzai and Kadonaga observed for SMARCAL1 (15). Alternatively, SMARCAL1 may function similarly to the yeast anti-recombinase Srs2, a helicase that inhibits the accumulation of recombination proteins at replication forks (47). Srs2 acts by removing Rad51 from DNA (48,49); further studies are required to determine if SMARCAL1 can perform this function.

It is unclear whether loss of the DSB- and fork-binding activities of SMARCAL1 or an as-yet unknown cellular function of the protein is responsible for the symptoms of SIOD. There is apparently no cancer predisposition in patients with the disease and no obviously detectable defects in DNA repair (50), which is consistent with our inability to detect significant sensitivity to γ or UV irradiation in SMARCAL1-depleted U2OS cells (L.P. and H.F., unpublished data). It seems likely that if SMARCAL1 is functional at DSBs, it is largely redundant with another protein or proteins. Interestingly, short stature is a feature of SIOD, indicating that the complicated disease phenotype may be caused by defective cell proliferation in select tissues (51). Our data suggest that these cell proliferation defects could be a consequence of the collapse of replication forks in SMARCAL1-deficient cells. Consistent with this hypothesis, short stature is also present in Bloom syndrome, and Werner syndrome patients display slow growth (52). Further study will be required to definitively determine whether destabilized replication forks contribute to this or other aspects of SIOD phenotype.

REFERENCES

1. Hoeijmakers, J. H. (2001) *Nature* **411**, 366-374
2. Fanning, E., Klimovich, V., and Nager, A. R. (2006) *Nucleic Acids Res* **34**, 4126-4137
3. Mimitou, E. P., and Symington, L. S. (2009) *Trends Biochem Sci* **34**, 264-272
4. Zou, L., and Elledge, S. J. (2003) *Science* **300**, 1542-1548
5. Byun, T. S., Pacek, M., Yee, M. C., Walter, J. C., and Cimprich, K. A. (2005) *Genes Dev* **19**, 1040-1052
6. Pacek, M., and Walter, J. C. (2004) *EMBO J* **23**, 3667-3676
7. Paulsen, R. D., and Cimprich, K. A. (2007) *DNA Repair (Amst)* **6**, 953-966
8. Lopes, M., Cotta-Ramusino, C., Pellicioli, A., Liberi, G., Plevani, P., Muzi-Falconi, M., Newlon, C. S., and Foiani, M. (2001) *Nature* **412**, 557-561
9. Sogo, J. M., Lopes, M., and Foiani, M. (2002) *Science* **297**, 599-602
10. Postow, L., Ghenoiu, C., Woo, E. M., Krutchinsky, A. N., Chait, B. T., and Funabiki, H. (2008) *J Cell Biol* **182**, 467-479
11. Hockensmith, J. W., Wahl, A. F., Kowalski, S., and Bambara, R. A. (1986) *Biochemistry* **25**, 7812-7821

12. Coleman, M. A., Eisen, J. A., and Mohrenweiser, H. W. (2000) *Genomics* **65**, 274-282
13. Muthuswami, R., Truman, P. A., Mesner, L. D., and Hockensmith, J. W. (2000) *J Biol Chem* **275**, 7648-7655
14. Shaw, G., Gan, J., Zhou, Y. N., Zhi, H., Subburaman, P., Zhang, R., Joachimiak, A., Jin, D. J., and Ji, X. (2008) *Structure* **16**, 1417-1427
15. Yusufzai, T., and Kadonaga, J. T. (2008) *Science* **322**, 748-750
16. Boerkoel, C. F., Takashima, H., John, J., Yan, J., Stankiewicz, P., Rosenbarker, L., Andre, J. L., Bogdanovic, R., Burguet, A., Cockfield, S., Cordeiro, I., Frund, S., Illies, F., Joseph, M., Kaitila, I., Lama, G., Loirat, C., McLeod, D. R., Milford, D. V., Petty, E. M., Rodrigo, F., Saraiva, J. M., Schmidt, B., Smith, G. C., Spranger, J., Stein, A., Thiele, H., Tizard, J., Weksberg, R., Lupski, J. R., and Stockton, D. W. (2002) *Nat Genet* **30**, 215-220
17. Spranger, J., Hinkel, G. K., Stoss, H., Thoenes, W., Wargowski, D., and Zepp, F. (1991) *J Pediatr* **119**, 64-72
18. Murray, A. W. (1991) *Methods Cell Biol* **36**, 581-605
19. Wohlschlegel, J. A., Dwyer, B. T., Dhar, S. K., Cvetic, C., Walter, J. C., and Dutta, A. (2000) *Science* **290**, 2309-2312
20. Rivera, T., and Losada, A. (2009) *Chromosoma* **118**, 223-233
21. Matsumoto, K., Aoki, K., Dohmae, N., Takio, K., and Tsujimoto, M. (2000) *Nucleic Acids Res* **28**, 4689-4697
22. Leach, C. A., and Michael, W. M. (2005) *J Cell Biol* **171**, 947-954
23. Golub, E. I., Gupta, R. C., Haaf, T., Wold, M. S., and Radding, C. M. (1998) *Nucleic Acids Res* **26**, 5388-5393
24. Brosh, R. M., Jr., Orren, D. K., Nehlin, J. O., Ravn, P. H., Kenny, M. K., Machwe, A., and Bohr, V. A. (1999) *J Biol Chem* **274**, 18341-18350
25. Shen, J. C., Lao, Y., Kamath-Loeb, A., Wold, M. S., and Loeb, L. A. (2003) *Mech Ageing Dev* **124**, 921-930
26. Doherty, K. M., Sommers, J. A., Gray, M. D., Lee, J. W., von Kobbe, C., Thoma, N. H., Kureekattil, R. P., Kenny, M. K., and Brosh, R. M., Jr. (2005) *J Biol Chem* **280**, 29494-29505
27. Mer, G., Bochkarev, A., Gupta, R., Bochkareva, E., Frappier, L., Ingles, C. J., Edwards, A. M., and Chazin, W. J. (2000) *Cell* **103**, 449-456
28. Unsal-Kacmaz, K., Chastain, P. D., Qu, P. P., Minoo, P., Cordeiro-Stone, M., Sancar, A., and Kaufmann, W. K. (2007) *Mol Cell Biol* **27**, 3131-3142
29. O'Neill, T., Dwyer, A. J., Ziv, Y., Chan, D. W., Lees-Miller, S. P., Abraham, R. H., Lai, J. H., Hill, D., Shiloh, Y., Cantley, L. C., and Rathbun, G. A. (2000) *J Biol Chem* **275**, 22719-22727
30. Matsuoka, S., Ballif, B. A., Smogorzewska, A., McDonald, E. R., 3rd, Hurov, K. E., Luo, J., Bakalarski, C. E., Zhao, Z., Solimini, N., Lerenthal, Y., Shiloh, Y., Gygi, S. P., and Elledge, S. J. (2007) *Science* **316**, 1160-1166
31. Kim, S. T., Lim, D. S., Canman, C. E., and Kastan, M. B. (1999) *J Biol Chem* **274**, 37538-37543
32. Smith, E., Dejsuphong, D., Balestrini, A., Hampel, M., Lenz, C., Takeda, S., Vindigni, A., and Costanzo, V. (2009) *Nat Cell Biol* **11**, 278-285
33. Jazayeri, A., Falck, J., Lukas, C., Bartek, J., Smith, G. C., Lukas, J., and Jackson, S. P. (2006) *Nat Cell Biol* **8**, 37-45
34. Branzei, D., and Foiani, M. (2009) *DNA Repair (Amst)*
35. Lisby, M., Barlow, J. H., Burgess, R. C., and Rothstein, R. (2004) *Cell* **118**, 699-713
36. Meister, P., Taddei, A., Vernis, L., Poidevin, M., Gasser, S. M., and Baldacci, G. (2005) *J Cell Biol* **168**, 537-544
37. San Filippo, J., Sung, P., and Klein, H. (2008) *Annu Rev Biochem* **77**, 229-257
38. Morrison, A. J., Highland, J., Krogan, N. J., Arbel-Eden, A., Greenblatt, J. F., Haber, J. E., and Shen, X. (2004) *Cell* **119**, 767-775
39. Park, J. H., Park, E. J., Lee, H. S., Kim, S. J., Hur, S. K., Imbalzano, A. N., and Kwon, J. (2006) *EMBO J* **25**, 3986-3997

40. Bachrati, C. Z., and Hickson, I. D. (2008) *Chromosoma* **117**, 219-233
41. Liberi, G., Maffioletti, G., Lucca, C., Chiolo, I., Baryshnikova, A., Cotta-Ramusino, C., Lopes, M., Pellicioli, A., Haber, J. E., and Foiani, M. (2005) *Genes Dev* **19**, 339-350
42. Ralf, C., Hickson, I. D., and Wu, L. (2006) *J Biol Chem* **281**, 22839-22846
43. Machwe, A., Xiao, L., Groden, J., and Orren, D. K. (2006) *Biochemistry* **45**, 13939-13946
44. Machwe, A., Xiao, L., Lloyd, R. G., Bolt, E., and Orren, D. K. (2007) *Nucleic Acids Res* **35**, 5729-5747
45. Cheok, C. F., Wu, L., Garcia, P. L., Janscak, P., and Hickson, I. D. (2005) *Nucleic Acids Res* **33**, 3932-3941
46. Garcia, P. L., Liu, Y., Jiricny, J., West, S. C., and Janscak, P. (2004) *EMBO J* **23**, 2882-2891
47. Burgess, R. C., Lisby, M., Altmannova, V., Krejci, L., Sung, P., and Rothstein, R. (2009) *J Cell Biol* **185**, 969-981
48. Krejci, L., Van Komen, S., Li, Y., Villemain, J., Reddy, M. S., Klein, H., Ellenberger, T., and Sung, P. (2003) *Nature* **423**, 305-309
49. Veaute, X., Jeusset, J., Soustelle, C., Kowalczykowski, S. C., Le Cam, E., and Fabre, F. (2003) *Nature* **423**, 309-312
50. Boerkoel, C. F., O'Neill, S., Andre, J. L., Benke, P. J., Bogdanovic, R., Bulla, M., Burguet, A., Cockfield, S., Cordeiro, I., Ehrich, J. H., Frund, S., Geary, D. F., Ieshima, A., Illies, F., Joseph, M. W., Kaitila, I., Lama, G., Leheup, B., Ludman, M. D., McLeod, D. R., Medeira, A., Milford, D. V., Ormala, T., Rener-Primec, Z., Santava, A., Santos, H. G., Schmidt, B., Smith, G. C., Spranger, J., Zupancic, N., and Weksberg, R. (2000) *Eur J Pediatr* **159**, 1-7
51. Clewing, J. M., Antalfy, B. C., Lucke, T., Najafian, B., Marwedel, K. M., Hori, A., Powel, R. M., Do, A. F., Najera, L., SantaCruz, K., Hicks, M. J., Armstrong, D. L., and Boerkoel, C. F. (2007) *J Med Genet* **44**, 122-130
52. Bohr, V. A. (2008) *Trends Biochem Sci* **33**, 609-620

FOOTNOTES

We thank W.M. Michael, R. Rothstein, M. Jasin, T. de Lange, D. Shechter, E. Foley, and members of the Funabiki lab for helpful discussions. We thank A. Krutchinsky for the use of equipment, B. Houghtaling and J.R. Hogg for technical advice, and C. Zierhut for reading the manuscript. We thank E. Foley, T. Kapoor, and W.M. Michael for reagents. L.P. was supported by a fellowship from the Leukemia and Lymphoma Society of America and by National Research Service Award CA09673. E.M.W. was supported by a Howard Hughes Medical Institute predoctoral award. B.T.C. was supported by NIH grant RR00862. H.F. was supported by the Rockefeller University and the Irma T. Hirschl/Monique Weill-Caulier Trust.

The abbreviations used are: SIOD, Schimke immuno-osseous dysplasia; DSB, double-strand break; ssDNA, single-stranded DNA; RPA, replication protein A; MS, mass spectrometry; SMARCAL1, SWI/SNF related, matrix associated, actin dependent regulator of chromatin, subfamily a-like 1; dsDNA, double-stranded DNA; MS/MS, Tandem MS; SB, single biotin; DB, double biotin; SH, single hairpin; DH, double hairpin; DS, double strand; SS, single strand; WRN, Werner syndrome helicase; BLM, Bloom syndrome helicase; HU, hydroxyurea.

FIGURE LEGENDS

Fig. 1. Identification and confirmation of xSMARCAL1 as a DSB-binding protein. *A.* Cartoon representation of DNA structures used in this study. Biotinylated nucleotides were added to one or both ends of restriction enzyme-digested pBluescriptSK+ (3 kb) using the Klenow fragment of DNA

polymerase I. Biotinylated DNA was then bound to streptavidin-coated magnetic beads. When one end contained biotinylated nucleotides (SB-DNA), the exposed end resembled a DSB. When both ends were biotinylated (DB-DNA), they were obscured by the bead. Additional DNA structures were constructed using biotinylated oligonucleotides. The SH-DNA structure is a 4-nucleotide biotinylated hairpin on a 20 bp stem, and the DH-DNA is identical except that the end is capped with a second 4-nucleotide hairpin. The DS-DNA is the product of annealing two 49-mer complimentary oligos, one of which contains biotin at its 3' end. SS-DNA is a 48-mer that contains biotin at its 3' end. SB-DNA and DB-DNA are shown bound to a streptavidin-coated bead. For all other DNAs, biotin is depicted by an encircled "B". *B.* Following the identification of xSMARCAL1 by tandem mass spectrometry, in vitro-translated xSMARCAL1 and histone H3 were added to CSF egg extract, allowed to bind to streptavidin-coated (SA), SB-DNA (SB), or DB-DNA (DB) beads, and interacting proteins were analyzed using a phosphorimager. While the control H3 binds equally well to SB-DNA and DB-DNA beads, xSMARCAL1 has a clear preference for SB-DNA beads. *C.* In contrast to the preference of xSMARCAL1 for SB-DNA beads, the chromatin remodeler xSNF2L showed no preference. *D.* SB-DNA (SB), DB-DNA (DB), SH-DNA (SH), DH-DNA (DH), DS-DNA (DS), and SS-DNA (SS) beads were incubated in egg extract for 30 minutes, after which associated proteins were isolated and analyzed by immunoblot. To control for DNA structural elements, immunoblots were probed with antibodies against xKu70, xCIRP2, and H3.

Fig. 2. hSMARCAL1 forms damage-dependent foci that colocalize with hRPA. *A.* U2OS cells expressing hSMARCAL1-GFP were treated with 10 Gy γ irradiation, fixed at indicated timepoints, and analyzed by immunofluorescence using a mouse anti-GFP antibody. Characteristic cells containing foci are shown. Bar: 10 μM. *B.* Cells expressing hSMARCAL1-GFP were treated with 10 Gy irradiation, fixed after 10 hours, and analyzed by immunofluorescence using mouse anti-γH2AX and rabbit anti-GFP, rabbit anti-hRAD51 and mouse anti-GFP, or mouse anti-hRPA32 and rabbit anti-GFP antibodies. hSMARCAL1-GFP and hRPA32 colocalize, as seen by an expansion of the boxed regions. Bar: 10 μM. *C.* Quantification of colocalization of DNA damage marker foci with hSMARCAL1-GFP foci. Among all detectable γH2AX (n = 74 cells), hRAD51 (n = 69 cells), and hRPA32 (n = 81 cells) foci, the fraction (%) of those that colocalized with hSMARCAL1-GFP was measured for each cell. Distribution of the colocalization frequency is shown.

Fig. 3. SMARCAL1 colocalizes with RPA at stalled replication forks. *A.* Sperm nuclei (4000 /μl) were incubated with interphase egg extract to allow for chromosomal replication. Geminin was added before the addition of chromatin to inhibit replication initiation, and aphidicolin was added 15 minutes after addition of chromatin to stall replication forks, as indicated. Chromatin was enriched by spinning through a 30% sucrose cushion after a one-hour total incubation. Co-sedimenting proteins were analyzed by immunoblot. As a control, extract was incubated in the absence of sperm chromatin but otherwise treated identically. Ub: mono-ubiquitylated PCNA, resulting from DNA replication; di-Ub: di-ubiquitylated PCNA, resulting from stalled replication forks. *B.* Quantification of chromatin-binding xSMARCAL1 from three independent spin-down experiments. Error bars denote one standard deviation. *C.* Normally growing U2OS cells stably expressing hSMARCAL1-GFP were co-stained with antibodies against GFP and hRPA32. An expanded region demonstrates the colocalization. Bar: 10 μM. *D.* U2OS cells stably expressing hSMARCAL1-GFP were treated with 4 mM HU for 24 hours, then fixed and costained with anti-hRPA32 and anti-GFP antibodies. Bar: 10 μM. *E.* Quantification of colocalization of hRPA32 foci with hSMARCAL1-GFP foci. Among all detectable hRPA32 foci, the fraction (%) of those that colocalized with hSMARCAL1-GFP was measured for each cell. Distribution of the colocalization frequency is shown (n = 60 cells).

Fig. 4. xSMARCAL1 interacts with xRPA in egg extracts. *A.* Alignment of the N-terminus of SMARCAL1 with similar sequences in other proteins. The UNG2 and XPA sequences are known to

interact with the C-terminal domain of RPA32 (27). *B.* xSMARCAL1 was immunoprecipitated using an anti-xSMARCAL1 antibody or rabbit IgG as a control, and the isolated proteins were analyzed by immunoblot. I: input, SM: anti-xSMARCAL1 antibody. *C.* xSMARCAL1-FLAG translated in reticulocyte lysate or a control reticulocyte lysate reaction was mixed with egg extract and incubated with anti-FLAG antibodies. Isolated proteins were analyzed by immunoblot. *D.* xSMARCAL1 was depleted out of extract and reticulocyte lysate-expressed xSMARCAL1-FLAG or ΔN-xSMARCAL1-FLAG was added. The asterisk marks a non-specific band that interacts with the anti-xSMARCAL1 antibody. IVT: in vitro translated. These extracts were used for the experiments shown in *E* and *F*. *E.* FLAG-tagged full length (FL) or truncated (ΔN) xSMARCAL1 were immunoprecipitated using an anti-FLAG antibody, and isolated proteins were analyzed by immunoblot. *F.* xSMARCAL1-FLAG or ΔN-xSMARCAL1-FLAG were allowed to bind to SB-DNA or SH-DNA beads, and DNA-bound proteins were analyzed by immunoblot. Histone H3 and the ssDNA-binding protein xCIRP2 were used as DNA isolation controls for SB-DNA and SH-DNA beads respectively

Fig. 5. xSMARCAL1 and hSMARCAL1 are phosphorylated in response to the DNA damage checkpoint. *A.* Wild type xSMARCAL1 (WT), or a mutant version in which all 4 S/TQ sites were mutated to AQ (4AQ), was expressed in reticulocyte lysate, mixed with egg extract, allowed to bind to SB-DNA beads in the absence or presence of caffeine, and bound proteins were visualized using a phosphorimager. *B.* U2OS cells were grown in the presence or absence of 4 mM HU for 24 hours, and lysates were treated with λ phosphatase as indicated. *C.* hSMARCAL1 mobility was analyzed after U2OS cells grown in the presence or absence of caffeine were treated with or without 10 Gy irradiation (IR) and collected 24 hours later. Lysates were treated with λ phosphatase as indicated.

Fig. 6. hSMARCAL1-depleted cells have a higher frequency of hRAD51 foci following HU treatment. *A.* U2OS cells were treated with control non-targeting siRNAs (NT) or siRNAs targeting two distinct regions of the hSMARCAL1 gene (si#1 and si#2), and depletion was tested by immunoblot. More than 94% of the endogenous SMARCAL1 was depleted by either siRNA. *B.* Examples of two types of cells following HU treatment. U2OS cells were grown in the presence of 4 mM HU for 24 hours, fixed and probed with anti-hRAD51 and ani-hRPA32 antibodies. Representative cells displaying dim hRAD51 foci with hundreds of bright hRPA32 foci (top) and bright hRAD51 foci with fewer hRPA32 foci (bottom) are shown. The cells shown were treated with siRNA#3. Bar: 10 μM. *C.* U2OS cells were treated with nontargeting (NT) siRNAs or siRNAs targeting hSMARCAL1 (siRNA#1 and siRNA#2) and analyzed by immunofluoresence to determine the percent nuclei with greater than ten bright hRAD51 foci. The average of three independent experiments is shown, with standard deviations. n > 500 cells for each sample. *D.* Cells were treated with siRNAs and grown in 4 mM HU for 24 hours, after which cells with bright hRAD51 foci were counted. Significantly more hRAD51-positive nuclei were present in hSMARCAL1-depleted cells than in control cells. The average of three independent experiments is shown, with standard deviations. n > 500 cells for each sample.

Fig. 7. A model for SMARCAL1 function at stalled replication forks. SMARCAL1 binds at the single-strand/double-strand junction in the replicating arm, partially through an interaction between its N-terminus and the C-terminal domain of RPA32. In an ATP-dependent manner, it stabilizes base-pairing between the daughter and parent strands. In the absence of SMARCAL1, incomplete daughter strands are allowed to peel off their parent strands, leading to aberrant DNA structures and replication fork instability. Following a break at the fork, the end is resected, RAD51 is loaded, and the DNA enters the homologous recombination pathway.

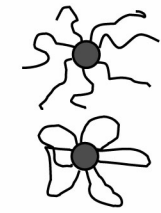

Single biotin DNA
(SB-DNA; 3 kb dsDNA)

Double biotin DNA
(DB-DNA; 3 kb dsDNA)

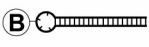

Single hairpin DNA
(SH-DNA; 20 bp dsDNA)

Double hairpin DNA
(DH-DNA; 20 bp dsDNA)

Double stranded DNA
(DS-DNA; 49 bp dsDNA)

Single stranded DNA
(SS-DNA; 48 nt ssDNA)

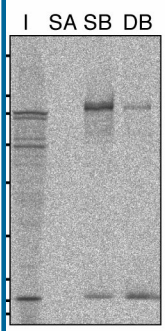

C

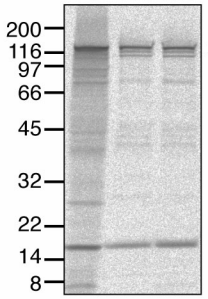

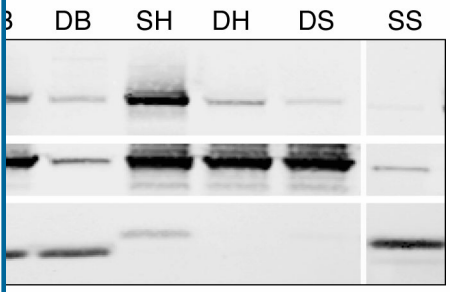

re 2

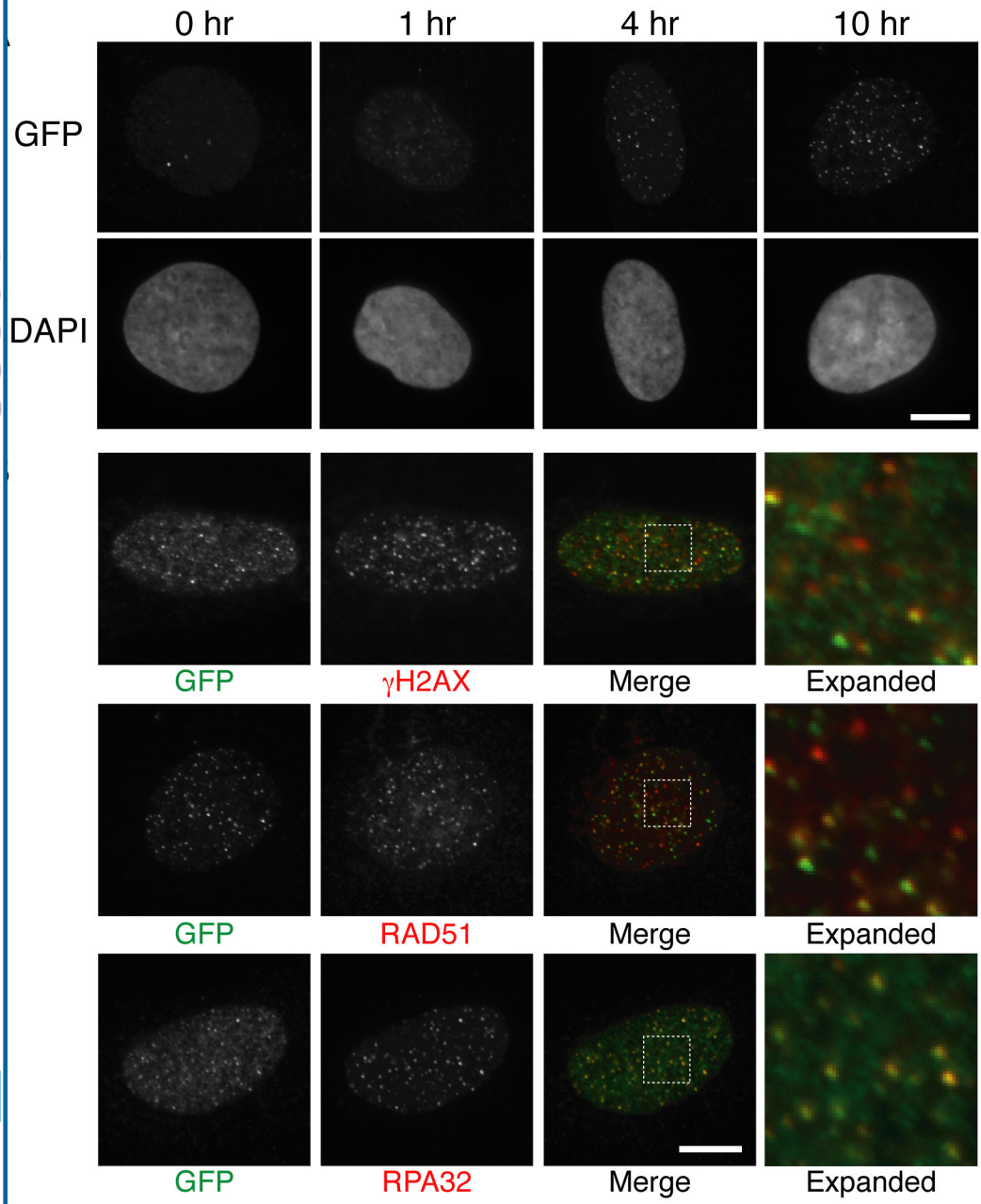
0 hr
1 hr
4 hr
10 hr
GFP
DAPI
GFP
γH2AX
Merge
Expanded
GFP
RAD51
Merge
Expanded
GFP
RPA32
Merge
Expanded

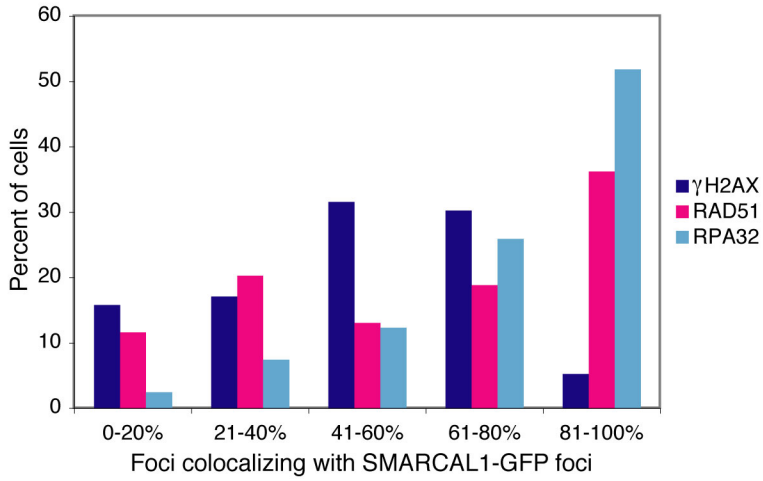
60
50
40
30
20
10
0
Percent of cells
0-20%
21-40%
41-60%
61-80%
81-100%
Foci colocalizing with SMARCAL1-GFP foci
γH2AX
RAD51
RPA32

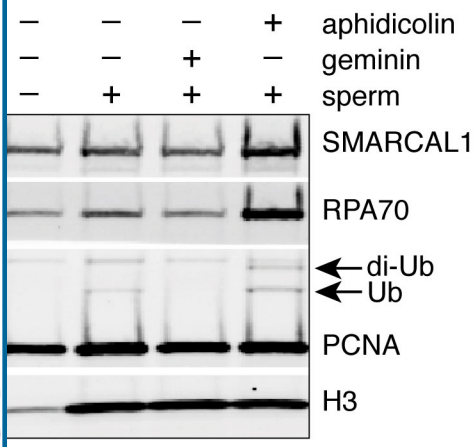
– – – + aphidicolin
– – + – geminin
– + + + sperm
SMARCAL1
RPA70
di-Ub
Ub
PCNA
H3

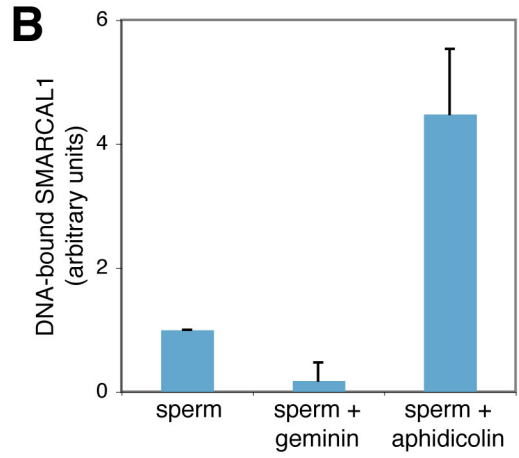
B
DNA-bound SMARCAL1 (arbitrary units)
0
2
4
6
sperm
sperm + geminin
sperm + aphidicolin

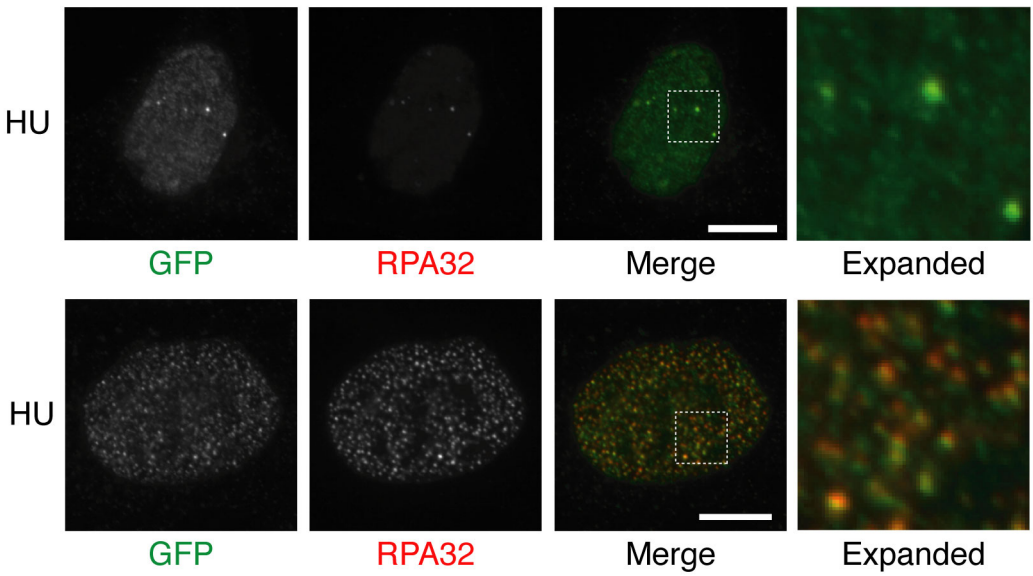
HU
GFP
RPA32
Merge
Expanded
HU
GFP
RPA32
Merge
Expanded

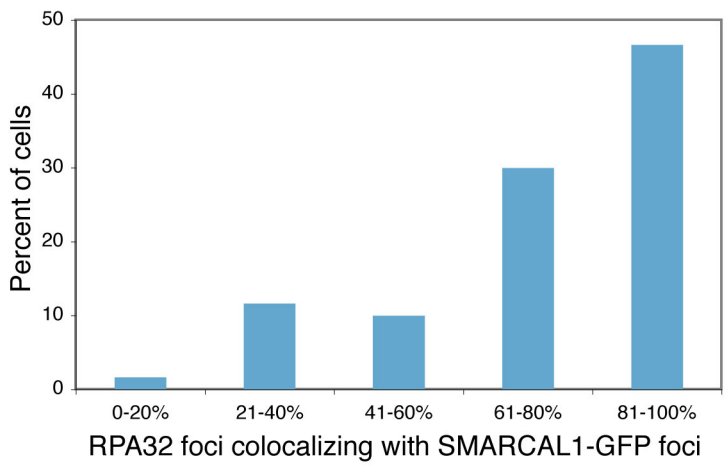
Percent of cells
0
10
20
30
40
50
0-20%
21-40%
41-60%
61-80%
81-100%
RPA32 foci colocalizing with SMARCAL1-GFP foci

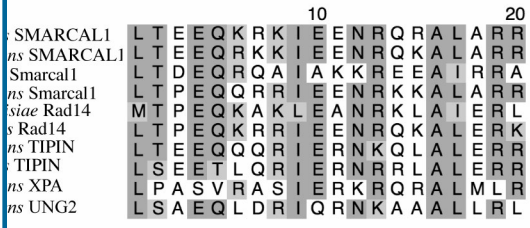
10
20
SMARCAL1 L T E E Q K R K I E E N R Q R A L A R R
ns SMARCAL1 L T E E Q R K K I E E N R Q K A L A R R
Smarcal1 L T D E Q R Q A I A K K R E E A I R R A
ns Smarcal1 L T P E Q Q R R I E E N R K K A L A R R
siae Rad14 M T P E Q K A K L E A N R K L A I E R L
s Rad14 L T P E Q K R R I E E N R Q K A L E R K
ns TIPIN L T E E Q Q Q R I E R N K Q L A L E R R
TIPIN L S E E T L Q R I E R N R R L A L E R R
ns XPA L P A S V R A S I E R K R Q R A L M L R
ns UNG2 L S A E Q L D R I Q R N K A A A L L R L

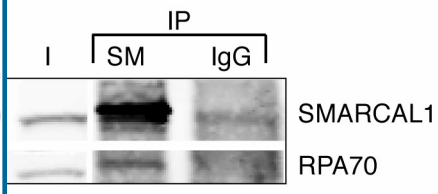
IP
I
SM
IgG
SMARCAL1
RPA70

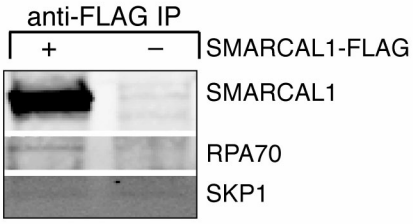
anti-FLAG IP
+
–
SMARCAL1-FLAG
SMARCAL1
RPA70
SKP1

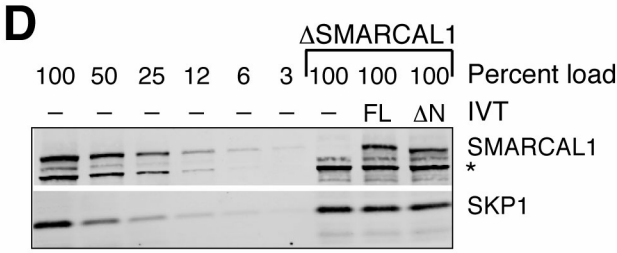
D
ΔSMARCAL1
100 50 25 12 6 3 100 100 100
Percent load
– – – – – – – FL ΔN
IVT
SMARCAL1
*
SKP1

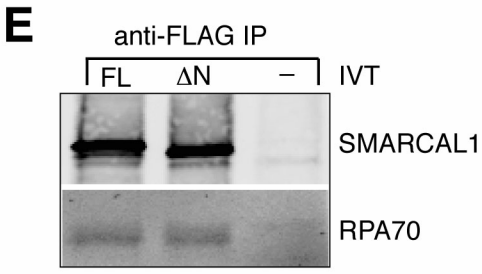
E
anti-FLAG IP
FL
ΔN
–
IVT
SMARCAL1
RPA70


F
DNA Beads
FL
ΔN
SB
SH
SB
SH
SMARCAL1
CIRP2
H3

ure 5

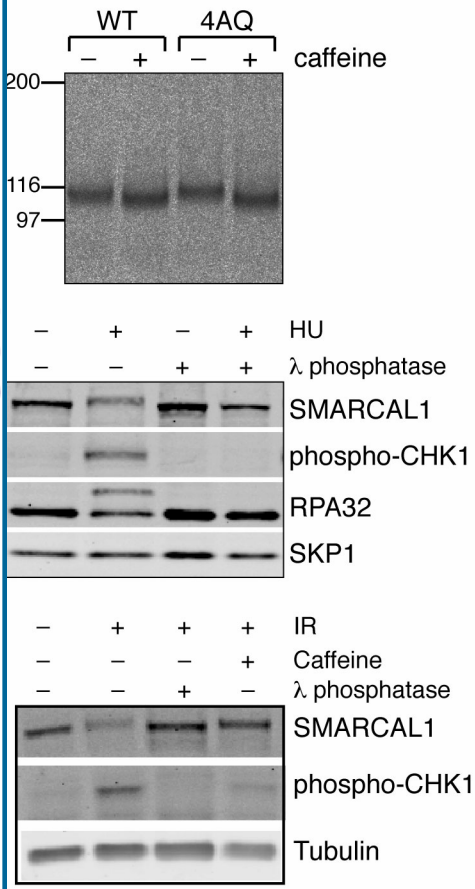

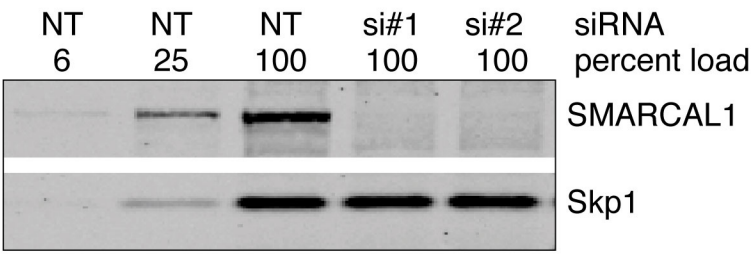
NT
6
NT
25
NT
100
si#1
100
si#2
100
siRNA
percent load
SMARCAL1
Skp1

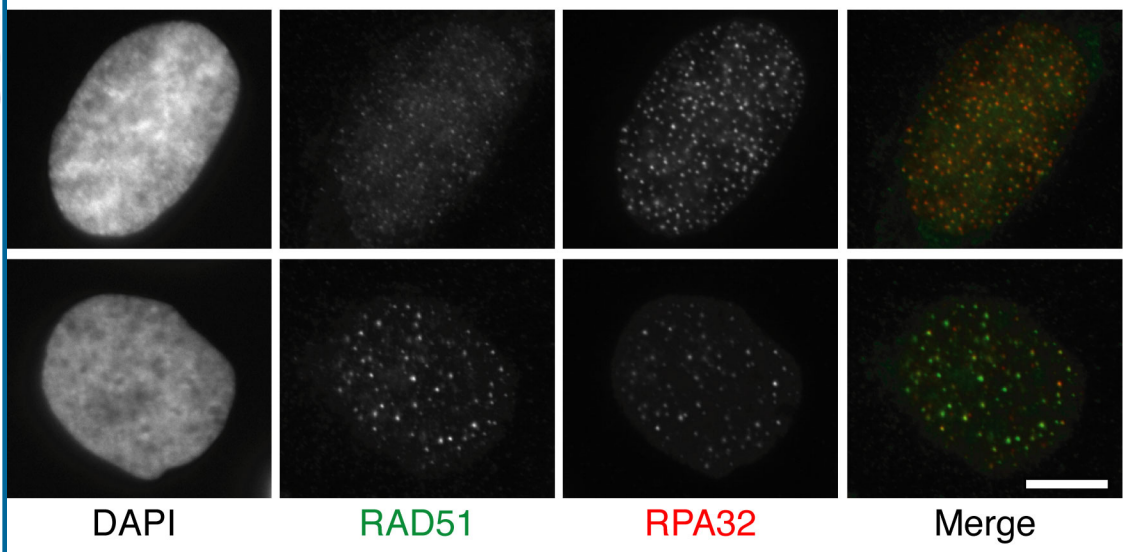
DAPI
RAD51
RPA32
Merge

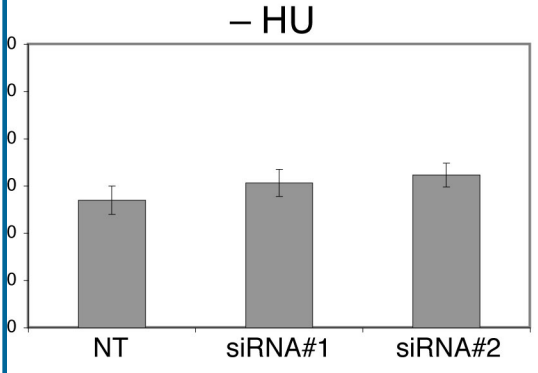
– HU
NT
siRNA#1
siRNA#2

D

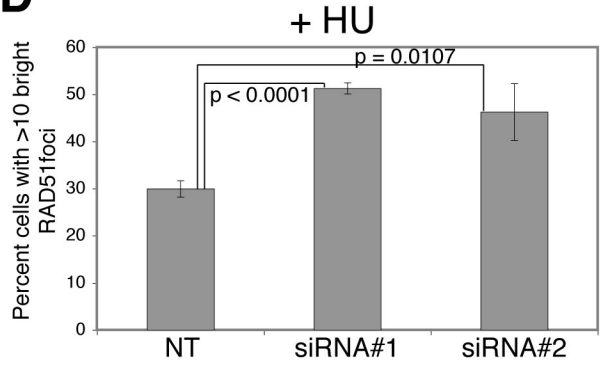
+ HU
p = 0.0107
p < 0.0001
Percent cells with >10 bright RAD51foci
60
50
40
30
20
10
0
NT
siRNA#1
siRNA#2

Figure 7